International Journal of Applied and Natural Sciences (IJANS)
ISSN (P): 2319-4014; ISSN (E): 2319-4022
Vol. 6, Issue 3, Apr - May 2017; 63 - 72

International Academy of Science, Engineering and Technology
Connecting Researchers; Nurturing Innovations

EFFECT OF ALUMINIUM AND TIN OXIDE DOPING ON THE STRUCTURAL AND OPTICAL PROPERTIES OF PULSED LASER DEPOSITED NANOCRYSTALLINE TANTALUM OXIDE THIN FILMS

RENJU R KRISHNAN

Department of Physics, St. Xavier's College, Thumba, Thiruvananthapuram, Kerala, India

ABSTRACT

Nanocrystalline SnO_2 and Al_2O_3 doped Ta_2O_5 thin films have been deposited on quartz substrates using reactive pulsed laser deposition. GIXRD studies indicate a phase transition from hexagonal δ- TaO to orthorhombic β-Ta_2O_5 for SnO_2 doped films around a substrate temperature of 773 K whereas the crystallization in the hexagonal δ- TaO phase for the Al_2O_3 doped films is found to be around 973 K. The preferred orientation is found to be sensitive to a substrate temperature for the SnO_2 doped films and is found to change from (0 0 1) to (110) crystal plane of the film deposited at a substrate temperature of 973 K. Micro Raman analysis of SnO_2 and Al_2O_3 doped films show a hardening and disappearance of certain modes which indicates a structural phase transition as confirmed from the GIXRD studies. Al_2O_3 doping gives rise to an additional mode around 150 cm^{-1} corresponding to O-Ta-O is bending vibrations in TaO_6 octahedra, which is found to be absent in SnO_2 doped films. The transmittance of Ta_2O_5 films deposited at 300 K is found to decrease up on SnO_2 doping and increase up on Al_2O_3 doping compared with the undoped film and decreases with the increase in substrate temperature for both dopants.

KEYWORDS: Micro-Raman Spectra, Pulsed Laser Deposition, Tantalum Oxide, Texture Coefficient, X-Ray Diffraction

INTRODUCTION

Tantalum oxide (Ta_2O_5) is an interesting material with very high dielectric constant ($\varepsilon_r \approx 25$), high refractive index ($n \approx 2.2$ @ $\lambda = 633$ nm), wide band gap ($E_g = 4.2$ eV) and transparent nature in a wide wavelength range from 300 nm to 2 μm [1]. It is widely used for applications like optical waveguides, interference filters, anti-reflection coatings, electroluminescent devices [2,3], corrosion barrier coatings, solid state oxygen sensors and thin film catalysts [4,5]. It has gained the attention as a memory dielectric, mainly due to the excellent step coverage characteristics and high dielectric constant combined with relatively low leakage currents enabling high values of charge storage [6]. In the chemical point of view, Ta_2O_5 is an interesting material, as the complexity of its crystal structure allows it to accommodate many different dopant ions in significant concentrations with only minor changes in crystal structure [7]. Ta_2O_5 possesses excellent chemical and thermal stability and promises good compatibility with standard microelectronic processing operations [8].

Ta_2O_5 films can be deposited by a number of techniques such as chemical vapour deposition [9], sol-gel synthesis [10], sputtering [11], electron beam evaporation [12], pulsed laser deposition [13-18], etc. The versatility of PLD lies in the fact that many experimental parameters like laser fluence, wavelength, pulse duration and repetition rate, preparation conditions, including target-to-substrate distance, substrate temperature, background gas and pressure, etc. can be altered,

which then have a strong influence on the film properties. Moreover in this method, since the energy source is located outside the chamber, use of ultra high vacuum (UHV) as well as ambient gas is possible [19].

In the present work, 5 wt. % aluminium oxide (Al_2O_3) and tin oxide (SnO_2) doped Ta_2O_5 films are deposited on quartz substrates using pulsed laser deposition. The films are grown at different substrate temperatures, viz., 300 (RT), 773, 873 and 973 K. The changes in the structural, morphological and optical properties of Ta_2O_5 films as a function of the two dopants and substrate temperatures are discussed in detail.

EXPERIMENTAL

Ta_2O_5 targets (undoped and doped individually with 5 wt. % of Al_2O_3 and SnO_2) are prepared by mixing dopant powder in to Ta_2O_5 powder. The powder is mixed in an agate mortar for 1h, pressed into 11 mm diameter and 3mm thickness pellet at 1.5 ton and then sintered at 900^0 C for 10 h in air. The deposition is carried out inside a stainless steel vacuum chamber equipped with a gas inlet and a substrate heater. The irradiations are performed using a *Q*- switched Nd:YAG laser (Quanta–Ray INDI – Series, Spectra Physics) with 200 mJ of laser energy at a frequency doubled 532 nm radiation having a pulse width of 7 ns and a repetition frequency of 10 Hz. Quartz plates held at a distance of 6.5 cm from the target in the on-axis geometry are used as the substrates. Deposition is done with a laser fluence 7 J/cm^2 for a duration of 15 minutes in oxygen atmosphere with back ground pressure of 2 x 10^{-3} mbar. Before irradiations, the deposition chamber is evacuated down to a base pressure of 5 x10^{-6} mbar. Films are deposited at different substrate temperatures, viz., 300, 773, 873 and 973 K. The crystallinity of the deposited films were studied with the help of Grazing incidence X-ray diffraction (GIXRD) measurements (Siemens D5000 Diffractometer) using Cu-Kα radiation at 1.5406 A^0. Data are collected at a scan rate of 1^0/minute. The surface morphology and surface roughness of the films were studied using atomic force microscopy (Si_3N_4 100 µ cantilever, 0.58 N/m force constant, contact mode Digital Instruments Nanoscope III). Grain size and root mean square (rms) surface roughness of the deposited films are determined on a scan area of 1 µm x 1 µm. The optical transmission and absorption spectra of the films were recorded using UV-VIS-NIR spectrophotometer (JASCO V-550) in the spectral range of 275-900 nm. Micro Raman spectra of the films are recorded using Labram-HR 800 Spectrometer equipped with excitation source laser radiation at λ=488 nm from an argon-ion laser. Spectra are acquired by a 1800 greeds/mm grating, a super-notch filter having a cut-off at 50 cm^{-1} and a Peltier cooled CCD camera, allowing a spectral resolution of about 1 cm^{-1}.

RESULTS AND DISCUSSIONS

Undoped Ta_2O_5 films deposited at substrate temperatures (T_s) up to 973 K are found to be amorphous in nature and is found to be in good agreement with the similar result of Mingfei et.al [15]. Figure 1 shows the GIXRD spectra of SnO_2 doped films deposited at different substrate temperatures. The film deposited at 300 K is found to have growth along the (001) plane confirming the hexagonal δ-TaO structure (JCPDS card no. 19-1299). The absence of another characteristic plane (100) for δ-TaO phase in SnO_2 doped films can be due to the presence of a large number of vacant lattice sites and local lattice disorders in the films which leads to obvious reduction in intensities or even the disappearance of the XRD peaks of some lattice planes [20].

XRD pattern of the film deposited at 773 K show the characteristic peaks of the orthorhombic Ta_2O_5 phase (JCPDS card no. 89-2843) showing the possibility of phase transition in this temperature range. For the orthorhombic Ta_2O_5 phase (110) is the reported preferred orientation. However in the SnO_2 doped films, deposited up to T_s=973 K, the

grains are grown along the preferred orientation of (001) plane. This observed phase modification and improved crystalline nature was not reported earlier for Ta_2O_5. The exact mechanism which results in the crystallization and phase transition of SnO_2 doped Ta_2O_5 films is still unknown, but it can be considered as the effect of SnO_2 doping which triggers the crytallization and recrystallization processes in Ta_2O_5. An indepth analysis of the crystal structure of Ta_2O_5 may be required to account for the reason of the observed phenomenon which is very difficult due to its complex structure. The crystallinity increased for the film deposited at T_s=873 K in terms of the increase in intensity of the diffracted peaks. Also a new peak along (111) plane is found to evolve for the film deposited at 873 K. For the film deposited at T_s=973 K, the intensity of the diffraction peaks is found to decrease compared to that deposited at 873 K and also the preferred orientation changes from (001) to (110) plane which is similar to the data given by JCPDS Card No. 89-2843. The intensity of the peak along (202) plane remains almost the same irrespective of the substrate temperature. It thus follows that good crystalline Ta_2O_5 films are formed at a substrate temperature of 873 K up on SnO_2 doping. Thus it can be concluded that SnO_2 is a good candidate for inducing crystallization in Ta_2O_5 thin films at smaller temperatures compared to undoped Ta_2O_5 films which remained amorphous even for a substrate temperature of 973 K.

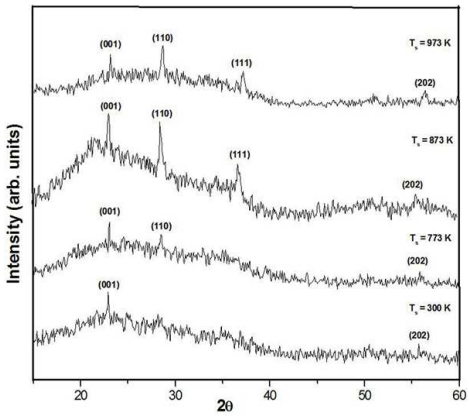

Figure 1: GIXRD Spectra of SnO_2 Doped Films at Different Substrate Temperatures

Figure 2 shows the variation of FWHM and grain size as a function of substrate temperature. The grain size calculation of the films using Scherrer formula, $D= 0.9\ \lambda/\beta\ \cos\theta$, where λ is the wavelength of X-rays, θ is the Bragg's angle of the XRD peak and β is the FWHM of the peak [21], reveals that the size of the particle increases from 38.6 nm for the films deposited at 300 K to 60 nm for the films deposited at 773 K and there after it decreases and then slightly increases for that deposited at 973 K. The grain size of the films deposited at 873 and 973 K are 18.29 and 21.5 nm respectively.

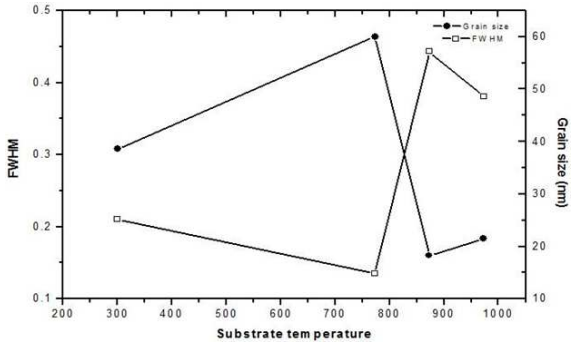

Figure 2: FWHM and Grain Size Variation of SnO_2 Doped Films as a Function of Substrate Temperature

To describe the preferred orientation, the texture coefficient TC(h k l), is calculated using the expression [22]

$$TC(hkl) = \frac{I(hkl)/I_0(hkl)}{N^{-1}\sum I(hkl)/I_0(hkl)}$$

where $I(h\ k\ l)$ is the measured relative intensity of a plane ($h\ k\ l$) and $I_0(h\ k\ l)$ is the standard intensity of the plane ($h\ k\ l$) taken from the JCPDS data. The value $TC(h\ k\ l) = 1$ represents films with randomly oriented crystallites, while higher values indicate the abundance of grains oriented in a given ($h\ k\ l$) direction. It indicates the maximum preferred orientation of the films along the diffraction plane meaning that the increase in preferred orientation is associated with the increased number of grains along that plane. Figure 3 depicts the variation of TC (0 0 1) and TC (110) of SnO_2 doped Ta_2O_5 films with substrate temperature. It is found from the plot that the preferred orientation is sensitive to substrate temperature. The preferred orientation of the film changes from (0 0 1) to (110) crystal plane for the film deposited at a substrate temperature of 973 K.

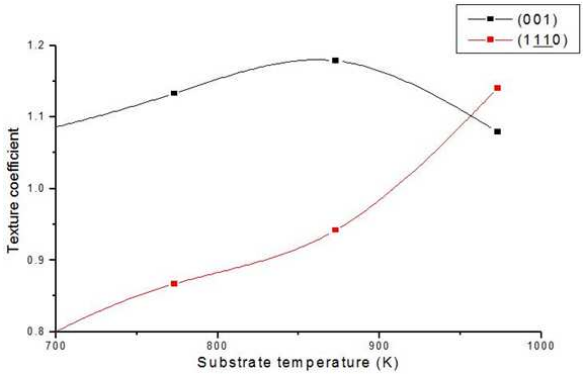

Figure 3: Texture Coefficient Variation of (001) and (1$\underline{1}$0) Planes as a Function of Substrate Temperature

Figure 4 shows the GIXRD spectra of Al_2O_3 doped films at different substrate temperatures. Al_2O_3 doped Ta_2O_5 deposited at room temperature and at substrate temperatures 773 K and 873 K are found to be amorphous. Doped films deposited at 973 K are found to be crystallizing in the δ-TaO hexagonal structure. In the reported XRD pattern (JCPDS card No. 19-1299) of Ta_2O_5 the peaks at (001) and (100) show 100 % intensity. But in the present case the peak along (100) plane appear with lesser intensity compared to the peak at (001). It is to be noted that the peak corresponding to (100) plane is absent in SnO_2 doped films. Particle size of Al_2O_3 doped films is found to be 54 nm for the film deposited at 973 K.

From the GIXRD analysis, it follows that SnO_2 doping is more efficient in enhancing crystallization in Ta_2O_5 films compared to Al_2O_3 doping, as the former becomes crystalline even at room temperature. Also the presence of SnO_2 induces a phase transition in Ta_2O_5 which is found to be absent in Al_2O_3 doped films. The above observations indicate that the structural properties of Ta_2O_5 films are sensitive to the dopants. The particle size is found to be smaller for SnO_2 doped films (except for the film deposited at 773 K) than that for Al_2O_3 doped films indicating that still smaller particles in the nanoregime can be synthesized by the precise control of deposition parameters for SnO_2 doped Ta_2O_5 films.

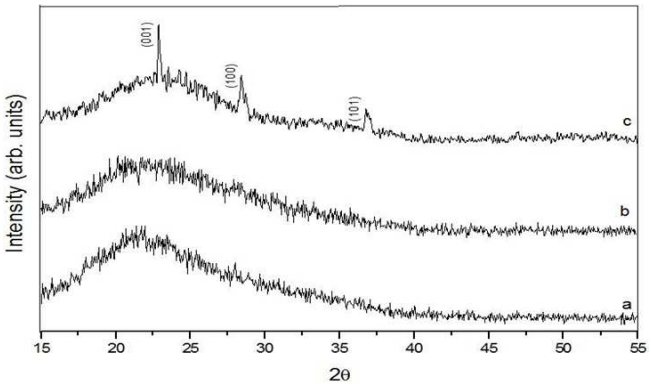

Figure 4: GIXRD Spectra of Al_2O_3 Doped Ta_2O_5 Films Deposited at (a) 300, (b) 873 and (d) 973 K

Figure 5 shows the Raman spectra of undoped Ta_2O_5 deposited at RT and SnO_2 doped Ta_2O_5 deposited at different substrate temperatures. The peaks at 489, 602 and 811 cm^{-1} are associated with the coupled modes involving mainly the stretching of various Ta-O bonds present in the structure with different magnitudes of bond order [23]. The characteristic bands of SnO_2 is found to be absent in the above spectra. As in the case of undoped Ta_2O_5 film, the bands at around 490, 670 and 819 cm^{-1} observed for the doped films indicates coupled modes involving mainly the stretching of various Ta-O bonds present in the structure with different magnitudes of bond order [23]. The mid energy Raman bands ($100 < \upsilon < 450$ cm^{-1}) at about 240 cm^{-1} found in the doped Ta_2O_5 films generally correspond to O-Ta-O bending vibrations in TaO_6 octahedra [23]. Thus it can be inferred that the band at about 240 cm^{-1} which was absent in the undoped Ta_2O_5 is present in SnO_2 doped Ta_2O_5 films. Low-energy phonon modes ($\upsilon < 100$ cm^{-1}) are also found to evolve in the doped films deposited at substrate temperatures more than RT. The modes at 242 and 813 cm^{-1} for the film deposited at 300 K show a hardening behaviour as the temperature increases to 773 K. This abrupt change in the hardening behaviour indicates a structural phase transition. Here this phase transition has been confirmed as the transition from hexagonal to orthorhombic phase of Ta_2O_5 for the films deposited at 773 K by XRD analysis. The present investigation clearly brings out the effect of SnO_2 doping on Ta_2O_5 films on the Raman spectra.

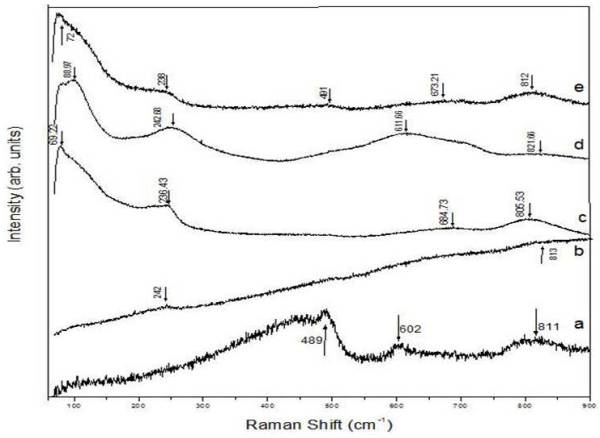

Figure 5: Micro-Raman Spectra of the (a) Undoped Film and SnO_2 Doped Films at Substrate Temperature(b) 300, (c) 773, (d) 873 and (e) 973 K

The micro-Raman analysis of the Al_2O_3 doped Ta_2O_5 deposited at different substrate temperatures show the presence of an additional mode at 150 cm^{-1} for the films deposited at 300 and 873 K. This mode corresponding to O-Ta-O bending vibrations in TaO_6 octahedra [23] was found to be absent in the undoped and SnO_2 doped films. A phase transition

of the amorphous films to hexagonal Ta_2O_5 phase can be inferred from the hardening and abrupt disappearance of the mode at 150 cm^{-1}. This fact has also been confirmed earlier by XRD studies. Figure 6 shows the micro-Raman spectra of Al_2O_3 doped films deposited at different substrate temperatures.

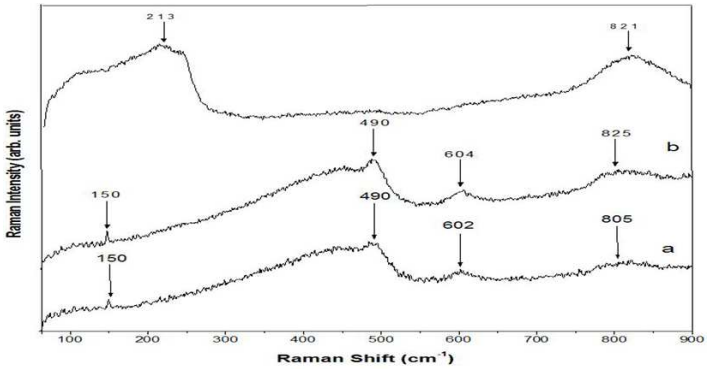

Figure 6: Micro-Raman Spectra of Al_2O_3 Doped Films at Substrate Temperature (a) 300, (b) 873 and (c) 973 K

Figure 7 shows the AFM micrographs for the SnO_2 doped films deposited at substrate temperatures of 873 and 973 K. The morphology of these films look like arrays of rods tied together and boundaries of the rods observed at 973 K stands well defined compared to that at 873 K. Rods of length about 300 nm and width 100 nm are found to be formed in the doped film deposited at 873 K. The length and width of these rods are found to increase slightly with the increase in substrate temperature to 973 K. No such rod formation is observed in the undoped film deposited at any substrate temperature (not shown here). Also for the doped films, rods are found to be formed only at higher substrate temperatures. The occurrence of these rods can be attributed to the presence of SnO_2 which all together changes the morphology of Ta_2O_5 films at higher substrate temperatures. The average rms roughness of the film deposited at 873 and 973 K is 49.3871 and 46.9627 nm.

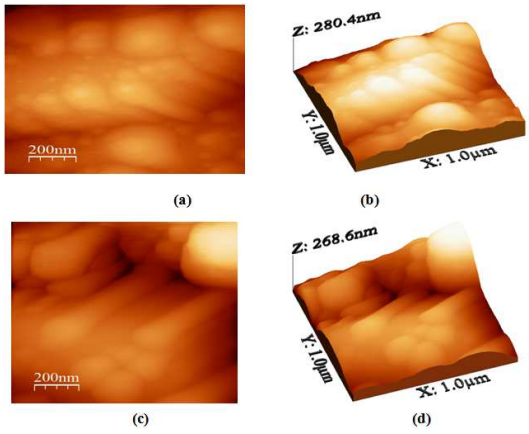

Figure 7: 2D and 3D AFM Micrographs of SnO_2 Doped Films Deposited at (a & b) 873 and (c & d) 973 K

The morphology of the Ta_2O_5 films change appreciably with Al_2O_3 doping as shown by AFM micrographs in Figure 8. The rod formation seen in the micrographs of SnO_2 doped films are found to be absent in Al_2O_3 doped films. Instead spherical particles, varying in size from 75 to 250 nm, are found to be formed with the increase in the substrate temperature.

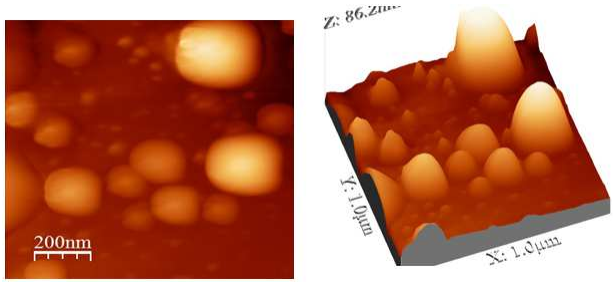

Figure 8: AFM Micrographs of Al_2O_3 Doped Films at 973 K (a) 2D, (b) 3D

Figure 9 shows the trasmittance spectra of the undoped film and SnO_2 doped films prepared at different substrate temperatures. The transmittance of the undoped film deposited at 300 K shows a maximum transmittance of 78 % at a photopic wavelength of 550 nm. The 550-nm wavelength indicates the peak of the photopic spectrum (human eye response spectrum). SnO_2 doping is found to reduce the transmittance of Ta_2O_5 films. For the doped film deposited at 300 K the transmittance is found to be 29 % which is very low compared to the undoped counterpart (78 %). A very low transmittance of 24% is observed for the film deposited at 973 K. This reduction in transmission of the doped films may be attributed to the enhanced absorption of Sn ions. The doped films appear dark in colour compared to the undoped one. The transmittance of the SnO_2:Ta_2O_5 films are found to be maximum, viz., 31 %, for deposition at 773K, the temperature at which the films crystallize in the orthorhombic form from the hexagonal phase. For the films deposited above 773 K, the transmittance decreases with increase in substrate temperature, and for that at 973 K, the transmittance is found to be 24 %. The decrease in transmittance of the doped films deposited above 773 K may be attributed to the transition to highly ordered orthorhombic phase from the less ordered hexagonal phase of Ta_2O_5.

In general, the decrease in the transmittances in films prepared at elevated substrate temperatures may be mainly as a result of insufficient incorporation of oxygen in the films during deposition. Kuster and Ebert [24] reported a similar result, an increase in the absorption in TiO_2 films with increasing substrate. They explained that on the basis of decomposition of TiO_2 at elevated temperatures. Therefore, the decrease in the transmittance in SnO_2 doped Ta_2O_5 films prepared at higher substrate temperatures may be due to the decomposition of Ta_2O_5 at elevated temperatures.

Quantitative values of bandgap energy (E_g) are evaluated using the relation [25]

$$\alpha = \frac{A}{h\upsilon}\left(h\upsilon - E_g\right)^n$$

where A is a constant, hυ is the incident photon energy, and the exponent n depends on the kind of optical transition. The nature of transition in the film can be determined by plotting $(\alpha h\upsilon)^{1/n}$ against photon energy hυ for suitable value of *n* which yields straight line behaviour. The band gap Eg is determined by plotting $(\alpha h\upsilon)^{1/n}$ against photon energy hυ for suitable value of n for which the graph is a straight line and the value of Eg is obtained by extrapolating the linear portion of the graph to intercept the photon energy axis. For crystalline materials, n can take values 1/2, 3/2, 2, or 3 for direct allowed, direct forbidden, indirect allowed and indirect forbidden transitions, respectively [25]. The best linear fit for $(\alpha h\upsilon)^{1/n}$ vs. hυ curve is obtained for n=1/2 indicating a direct allowed transition in the films. The band gap energy of the films is found to decrease from 4.76 to 4.26 eV, up on increasing the substrate temperature from 300 to 973 K.

Films deposited at higher substrate temperatures are found to have lower band gap. This may be due to the sharp edges in the crystalline films. The decrease in the direct band gap with increase in substrate temperature may also be due to the presence of internal electric fields associated with the defects present in the films; or it may be due to the action of atmospheric oxygen on the surface of the film, which produces an acceptor level in the forbidden band [26].

Figure 10 shows the transmittance spectra of Al_2O_3 doped films deposited at different substrate temperatures. A highly transparent Ta_2O_5 film with transmission as high as 91 % is obtained for the Al_2O_3 doped films deposited at 300 K. With the increase in the substrate temperature, the transmittance is found to decrease. The transmittance for the films deposited at 873 and 973 K is found to be 77 % and 45 %.

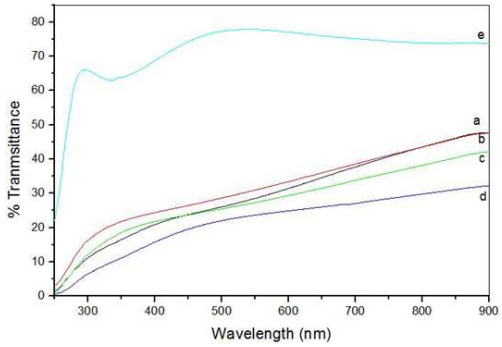

Figure 9: Transmittance Spectra of (a) Undoped Film and SnO_2 Doped Films at Substrate Temperature (b) 300, (c) 773, (d) 873 and (e) 973 K

The high transparency of the doped film deposited at 300 K may be due to the amorphous state of the film.

It can also be noted that the transmittance of Al_2O_3 doped film deposited at 300 K (91 %) is more than that of the undoped Ta_2O_5 film deposited at the same substrate temperature (78 %). At 973 K, the film crystallizes in the hexagonal Ta_2O_5 phase, a relatively ordered phase compared with the amorphous state, which results in the obvious reduction of transmittance.

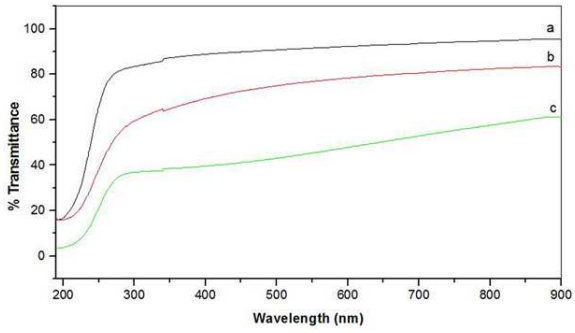

Figure 10: Transmittance Spectra of Al_2O_3 Films Deposited at (a) 300, (b) 873 and (c) 973 K

Here also, as in the previous case the decrease in the transmittance in Al_2O_3 doped Ta_2O_5 films prepared at higher substrate temperatures may be due to the decomposition of Ta_2O_5 at elevated temperatures. Another possible cause for the decrease in transmittance may be due to the increase in scattering of light with increase in substrate temperature. Due to this, the coherence between the primary light beam and the beams reflected between the film boundaries is lost and results in the disappearance of the interference which in turn decreases the transmittance [27].

The bandgap of Al_2O_3 doped Ta_2O_5 thin films are also estimated using the above said method by extrapolating straight line of $(\alpha h\nu)^{1/n}$ vs. $h\nu$ curve to the energy axis. As in the case of SnO_2 doped films, Al_2O_3 doping also gives the best linear fit for n=1/2, indicating a direct allowed transition. The bandgap values of the films are found to decrease from 4.4 to 3.3 eV with increase in substrate temperature.

CONCLUSIONS

High-quality Al_2O_3/SnO_2 doped Ta_2O_5 films are deposited on quartz substrates using pulsed laser deposition technique. SnO_2 doped films indicate a phase transition from hexagonal δ- TaO to orthorhombic β-Ta_2O_5 around a substrate temperature of 773 K, whereas the crystallization is found to be in the hexagonal δ- TaO phase for the Al_2O_3 doped films around 973 K. Texture coefficient of the SnO_2 doped films is found to be sensitive to substrate temperature and is found to change from (0 0 1) to (110) crystal plane for the film deposited at 973 K. Micro Raman analysis of SnO_2 and Al_2O_3 doped films show a hardening and disappearance of certain vibrational modes in the films. Al_2O_3 doping gives rise to an additional mode around 150 cm^{-1} corresponding to O-Ta-O bending vibrations in TaO_6 octahedra, which is found to be absent in SnO_2 doped films. AFM analysis reveals the strong dependence of morphology of the films on the nature of dopants; a rod-like structure formation for SnO_2 doped films, which is entirely different from the granular structure formation for the Al_2O_s doped ones. The transmittance and band gap of the films are also found to be sensitive to the dopants considered.

ACKNOWLEDGEMENTS

The author gratefully acknowledges the help rendered by DAE Inter University Consortium (IUC), Indore, India for the characterization studies of the films.

REFERENCES

1. Traylor Kruschwitz J. D and Powlewicz W. T // *Appl. Opt.* **36 (10) (**1997) 2157.
2. Doumuki T, Tamada H and Saitoh M // *Appl. Phys. Lett*. **64** (1994) 3533.
3. Pollard K.D and Puddephatt R.J // *Chem. Mater*. **11** (1999) 1069.
4. Ushikubo T // *Catal. Today* **57** (2000) 331.
5. Baltes M, Kytokivi A, Weckhuysen B. M, Schoonheydt R. A, Van Der Voort P and Vansant E.F// *J. Phys. Chem. B*1**05** (2001) 6211.
6. Atanassova E, Aygun G, Turan R and Babeva Tz // *J. Vac. Sci. Technol. A* **24 (2) (2006)** 206.
7. Cava R.J and Krajewski J.J // *J.Appl. Phys* **83 (3)** (1998) 1613.
8. Ezhilvalavan S and Tseng T. Y // *J. Mater. Sci.: Mater. Electron*. **10 (1) (**1999) 9.
9. Lee J. S, Chang S. J, Chen J. F, Sun S. C, Liu C. H and Liaw U. H // *Mat. Che Phys*. **77** (2002) 242.
10. Ndiege N, Wilhoite T, Subramanian V, Shannon M. A and Masel R. I // *Chem. Mater.*, **19** (2007) 3155.
11. Pai Y. H, Chou C. C and Shieu F. S // *Mat. Che Phys* **107 (**2008) 524.

12. Martin P. J, Bendavid A, Swain M, Netterfield R. P, Kinder T. J, Sainty W. G, Drage D and Wielunski L // *Thin Solid Films* **239 (**1994) 181.
13. Geretovszky Zs, Szorenyi T, Stoquert J.-P and Boyd I. W // *Thin Solid Films* **453-454** (2004) 245.
14. Hino T, Mustofa S, Nishida M and Araki T // *Vacuum* **70** (2003) 47.
15. Mingfei Z, Zhengwen F, Haijun Y, Zhuangjian Z and Qizong Q // *Appl. Surf. Sci*., **108** (1997) 399.
16. Nishimura Y, Shinkawa A, Ujita H, Tsuji M and Nakamura M // *Appl. Surf. Sci*. **136** (1998) 22.
17. Zhang J.-Y, Fang Q and Boyd I.W // *Appl. Surf. Sci*. **138-139** (1999) 320.
18. Boughaba S, Islam M, McCaffrey J. P, Sproule G. I, Graham M. J // *Thin Solid Films* **371** (2000) 119.
19. Chrisey D. B and Hubler G. K, *Pulsed Laser Deposition of Thin films* (Wiley, New York, 1994).
20. Chen Z. W, Lai J. K. L and Shek C. H // Phy. Rev. B **70** (2004) 165314.
21. Cullitty B. D, *Elements of X-ray Diffraction* (Addison Wesley, London, 1978).
22. Barret C and Massalki T. B, *Structure of Metals* (Pergamon, Oxford, 1980).
23. Dobal P. S, Katiyar R.S, Jiang Y, Guo R and Bhalla A.S // *J. Raman Spectrosc*. **31** (2000) 1061.
24. H. Kuster and J. Ebert // *Thin Solid Films* **70 (**1980) 43.
25. Pankove J. I, *Optical Processes in Semiconductors* (Dover, New York, 1971).
26. Koichi Kajihara, Katsuhisa Tanaka, Kazuyuki Hirao, and Naohiro Soga // *Jpn. Appl. Phys*. **35** (1996) 6110.
27. Meng L.J., Adritschky M., Dos Santos M.P // *Vacuum* **45** (1994) 19